Effect of autophagy on multiple myeloma cell viability

Bao Hoang, Angelica Benavides, Yijiang Shi, Patrick Frost, and Alan Lichtenstein

Department of Medicine, Division of Hematology-Oncology of the Greater Los Angeles Veterans Affairs Healthcare Center, University of California at Los Angeles Medical School, and the Jonsson Comprehensive Cancer Center, Los Angeles, California

Abstract

Because accumulation of potentially toxic malfolded protein may be extensive in immunoglobulin-producing multiple myeloma (MM) cells, we investigated the phenomenon of autophagy in myeloma, a physiologic process that can protect against malfolded protein under some circumstances. Autophagy in MM cell lines that express and secrete immunoglobulin and primary specimens was significantly increased by treatment with the endoplasmic reticulum stress–inducing agent thapsigargin, the mammalian target of rapamycin inhibitor rapamycin, and the proteasome inhibitor bortezomib. Inhibition of basal autophagy in these cell lines and primary cells by use of the inhibitors 3-methyladenine and chloroquine resulted in a cytotoxic effect that was associated with enhanced apoptosis. Use of small interfering RNA to knock down expression of beclin-1, a key protein required for autophagy, also inhibited viable recovery of MM cells. Because the data suggested that autophagy protected MM cell viability, we predicted that autophagy inhibitors would synergize with bortezomib for enhanced antimyeloma effects. However, the combination of these drugs resulted in an antagonistic response. In contrast, the autophagy inhibitor 3-methyladenine did synergize with thapsigargin for an enhanced cytotoxic response. These data suggest that autophagy inhibitors have therapeutic potential in myeloma but caution against combining such drugs with bortezomib. [Mol Cancer Ther 2009;8(7):1974–84]

Introduction

Recent work suggests it may be possible to exploit therapeutically the fact that multiple myeloma (MM) cells synthesize huge amounts of immunoglobulin (Ig). This invariably results in the presence of a significant amount of endoplasmic reticulum (ER)–localized unfolded or malfolded protein that is potentially toxic to the plasma cell. Indeed, the MM cell has exploited several molecular pathways to deal with this toxic protein and these are potential therapeutic targets. They include the proteasome (reviewed in ref. 1), up-regulated expression of heat shock protein chaperones (2), activation of the unfolded protein response (UPR) pathway (3–5), and aggresome formation (6, 7). The remarkable efficacy of the proteasome inhibitor bortezomib in MM cells and patients (8, 9) and the correlation of its *in vitro* effectiveness with amount of Ig expressed (3, 10) support the notion of targeting pathways that degrade or refold toxic malfolded proteins. Additional studies on the antimyeloma effects of heat shock protein inhibitors (2) and drugs that prevent aggresome formation (6, 7) are also consistent with this hypothesis.

The induction of autophagy is an additional potential pathway that might protect MM cells against toxic malfolded proteins and could be targeted. Autophagy is a degradation process of proteins and organelles in which double-membrane vesicles, termed autophagosomes, sequester cytosolic proteins and/or organelles (reviewed in ref. 11). Following vesicle fusion with lysosomes, the contents are degraded by hydrolases (12–14). Autophagy is essential for normal cell function and occurs at a basal level in all cells. Increased autophagy can be induced, most prominently by nutrient starvation or mammalian target of rapamycin (mTOR) inhibition, which shuts down protein translation. In those cases, following hydrolysis of autophagosomal cargo, the resulting macromolecules are presumably released from the vacuole for reuse to ameliorate the starvation effect. However, recent studies suggest that autophagy can also function to remove toxic aggregated proteins such as mutant huntingtin and α-synuclein (15–17). Furthermore, ER stress inducer stimulation of the UPR can up-regulate expression of autophagy-regulatory genes (18) and can activate autophagy via the downstream activation of IRE-1/c-Jun NH_2-terminal kinase (JNK) pathway (19) or the PERK/eIF2α pathway (20). These studies suggest that autophagy may be an important additional process by which the malignant plasma cell could protect itself from toxic malfolded Ig. We, thus, tested this notion in MM cell lines and primary specimens. A significant degree of autophagy was present in the basal state of these MM cells, and the proteasome inhibitor bortezomib, the ER stress inducer thapsigargin, and the mTOR inhibitor rapamycin were all capable of further increasing autophagy. Inhibiting autophagy with inhibitors and by silencing beclin-1, an important protein required for autophagy, resulted in a toxic effect on MM cells. Although we anticipated that blocking autophagy with inhibitors would synergize with the antimyeloma effects of bortezomib,

Received 12/15/08; revised 3/27/09; accepted 4/14/09; published OnlineFirst 6/9/09.

Grant support: NIH grants RO1CA111448 and KO1CA111623, Multiple Myeloma Research Foundation, and research funds of the Veteran's Administration.

The costs of publication of this article were defrayed in part by the payment of page charges. This article must therefore be hereby marked *advertisement* in accordance with 18 U.S.C. Section 1734 solely to indicate this fact.

Requests for reprints: Alan Lichtenstein, Hematology-Oncology, West Los Angeles Veterans Affairs Hospital, 11301 Wilshire Boulevard, Los Angeles, CA 90073. Phone: 310-478-3711, ext. 40021; Fax: 310-268-4508. E-mail: alan.lichtenstein@med.va.gov

doi:10.1158/1535-7163.MCT-08-1177

we found an antagonistic effect. In contrast, inhibiting autophagy synergized with thapsigargin for enhanced cytotoxicity and apoptosis. The data support the notion that inhibiting autophagy is a potential therapeutic maneuver in myeloma but that the complex interaction between autophagy and proteasome inhibition needs further study before considering combination therapy with autophagy inhibitors plus bortezomib.

Materials and Methods

Approval for these studies was obtained from the Greater Los Angeles Veterans Administration Healthcare System institutional review board. Informed consent was provided according to the Declaration of Helsinki.

Cell Lines and Primary Specimens

OPM-2, 8226, and U266 cell lines were purchased from the American Type Culture Collection and maintained in culture as previously described (21, 22). Primary malignant cells were isolated from bone marrow by positive selection for CD38 (>98% pure) as previously described (23).

Cell Survival and Apoptosis Assays

Survival assays were done as previously described (24). Surviving cells were enumerated by trypan blue exclusion. In individual experiments, groups were run in quadruplicate and the means of the replicates were used to calculate the percentage inhibition of viable recovery compared with untreated groups. The data are presented as percentage of control, means of three or more individual experiments. Apoptosis was identified by flow cytometric staining for expression of activated caspase-3 (BD Biosciences) as previously described (24).

Immunoblot Assays

Protein expression was assayed as previously described (24).

Transfections

The green fluorescent protein (GFP)-LC3 coding sequence was isolated from pEGFP-LC3 plasmid (kind gift of Dr. Hong-Gang Wang, Moffitt Cancer Center, Tampa, FL) by using primers SpeIGFPLC3 (5′-TTGCACTAGTATGGTGAGCAAGGGCGAGGAG-3′) and XhoIGFPLC3 (5′-GCTACTCGAGTTACACAGCCAGTGCTGTCCC-3′). SpeIGFPLC3XhoI PCR product was digested with *Spe*I and *Xho*I. Insert from pLenti6/V5IgGL vector was removed by *Spe*I/*Xho*I digestion and replaced with *Spe*I/*Xho*I-digested GFPLC3 to yield pLenti6GFPLC3. Lentivirus was produced according to Invitrogen's protocols. Briefly, pLenti6GFPLC3 was cotransfected with ViraPower DNA (Invitrogen) into 293 ft cells, and after 48 h, viral supernatant was collected. U266 and 8226 cells (2.5×10^5) were infected with 1 mL of viral supernatant overnight and then selected with 2.5 μg/mL blasticidin (Invitrogen) to generate stable cell lines. GFP-LC3 expression was confirmed by Western analysis.

To knock down beclin-1, U266 cells (2×10^6) were transfected with 1 μmol/L of Beclin SMARTpool small interfering RNA (siRNA; three separate siRNAs) or scramble duplex (purchased from Dharmacon) using the Amaxa Nucleofector II electroporation device and X005 program. Cells were then cultured in RPMI 1640 complete growth medium. For beclin protein knockdown analysis, cell lysates were collected after transfection, electrophoresed, and immunoblotted with anti-beclin antibody (Novus Biologicals).

Analysis of Autophagic Area by Fluorescent Microscopy

Autophagic area was assessed as previously described (19). Briefly, glass coverslips were coated with 0.01% poly-L-lysine (Sigma) in 24-well tissue culture plates overnight at 4°C and rinsed with PBS just before use. U266GFPLC3 or 8226GFPLC3 cells (20,000) were plated onto poly-L-lysine–coated coverslips in 500 μL of growth medium. After 2 h in culture, adherent cells were fixed with 3.7% formaldehyde for 10 min and rinsed with PBST (Tween 20). Cell membranes were permeabilized by treating with PBS/0.2% Triton X-100 for 5 min and rinsing with PBST. Cells were then blocked with PBST/10% normal goat serum, and anti-GFP antibody (JL-8 from Clontech) in blocking buffer was added at 4 μg/mL. After three washes with PBST, anti-mouse Alexa Fluor 488 secondary antibody (Molecular Probes) was added. Cells were additionally washed with PBST and coverslips were mounted on microscope slides in Prolong Gold antifade reagent (Invitrogen). Cells were visualized with a Leica Leitz DMRBE microscope using a 40× objective lens (Leica PL Fluotor) and fluorescent and corresponding bright-field images were captured (20 random fields/group) with a Hamamatsu C4742-95 camera and OpenLab program 3.1.5. Assays were done in blinded fashion. The images were transferred to NIH Image software and each cell was analyzed for total cell area (denominator) by outlining the perimeter of a bright-field image of the cell and quantifying the area inside. In addition, the corresponding fluorescent image of each cell was quantified for GFP-positive punctate area by density slice (numerator). For each cell, autophagic area is calculated as total punctate area divided by cell area (20 fields/group for each experiment). Data are presented as mean ± SD autophagic area of three separate experiments.

Electron Microscopy

After treatments, MM cells were fixed in phosphate buffer (pH 7.4) containing 2.5% glutaraldehyde and 2% paraformaldehyde at room temperature for 60 min. Cells were postfixed in 1% OsO_4 at room temperature for 60 min, dehydrated through graded ethanol solutions, and embedded in Quetol 812 (Nissin EM Co.). Sections were stained with uranyl acetate and lead citrate and examined with a transmission electron microscope. Autophagosomes were identified and quantitatively assessed as previously described (19). Data are presented as number of autophagosomes per cell, mean ± SD, $n = 20$.

Statistics

The effect of drug combinations on cytotoxicity was assessed by the median-effect method using CalcuSyn software, version 1.1.1 (Biosoft) as previously described (25). Combination index (CI) values were calculated using the most conservative assumption of mutually nonexclusive drug interactions. CI values were calculated from median

results of cytotoxicity assays, which were done in quadruplicate. CI values significantly >1 indicate drug antagonism. Linear regression correlation coefficients of the median-effect plots were required to be >0.90 to show that the effects of the drugs follow the law of mass action, which is required for a median-effect analysis.

The *t* test was used to determine significance of differences between groups.

Results

There Is Significant Basal Autophagy in MM Cells, Which Is Increased by Thapsigargin, Rapamycin, and Bortezomib

We were interested to see if induction of autophagy in MM cells occurs following treatment with thapsigargin, bortezomib, or rapamycin. Thapsigargin induces ER stress secondary to its inhibition of the Ca^{2+}-ATPase in the ER (26), which blocks sequestration of calcium by the ER, causing accumulation of unfolded proteins. As stated in Introduction, previous literature supports the notion that ER stress can induce autophagy. mTOR inhibitors such as rapamycin are well known to induce autophagy (27) and mTOR inhibitors have shown some potential antimyeloma efficacy in preclinical studies (28). Bortezomib is a clinically useful proteasome inhibitor that can also stimulate several components of the UPR (3, 4) and, thus, may also stimulate autophagy. We decided initially to study the U266, 8226, and OPM-2 MM cell lines because they are known to synthesize Ig molecules, which could sensitize them to autophagy inhibition. To assay autophagy in these MM cell lines, we attempted to stably express the LC3-GFP fusion protein in U266, 8226, and OPM-2 MM cells by lentiviral infection. We were successful in the U266 and 8226 cell lines. Microtubule-associated protein-1 LC3 is a component of mammalian autophagosomes, and thus, the GFP-LC3 fusion protein has been used as a reliable marker for their presence (29, 30). A punctate pattern of LC3 localization in the cell is characteristic of autophagosome formation and represents the accumulation of a membrane-bound form of LC3 onto autophagic vacuoles (30).

The U266 and 8226 cell lines are variably sensitive to cell death or cytostasis induced by thapsigargin, bortezomib, and rapamycin. Stable expression of LC3-GFP had no effect on the sensitivity of these cell lines to any of these three drugs (data not shown). Fluorescence analysis for LC3-GFP localization showed a significant amount of punctate staining in the nontreated MM cell lines, indicative of basal autophagosome formation. Constitutive expression of punctate LC3-GFP was seen in a very high percentage of 8226 and U266 cells (85% and 65%, respectively). It was, thus, difficult to show a statistically significant increase in punctate staining from drug treatment by simply enumerating positive versus negative cells. However, analysis of the autophagic area/cell (as described in Materials and Methods) clearly showed drug-stimulated enhancement of autophagy. As shown in Fig. 1A (*black columns*), approximately 2.5- to 3-fold increases were shown in both cell lines exposed to the drugs. The 8226 cell line treated with thapsigargin could not be analyzed as drug treatment prevented adherence of the cell line to coverslips, which was required for analysis.

Because measurement of "autophagic area" cannot distinguish between enlargement of autophagosomes versus an increase in numbers, we also analyzed the data for number of GFP-LC3 punctate signals per cell. These data also support a drug-induced increase in autophagosomes (Fig. 1A, *white columns*). The number of fluorescent autophagosomes in bortezomib- or rapamycin-treated 8226 cells (5.86 ± 0.47 and 4.39 ± 0.59, mean ± SE, $n = 45$) was significantly greater ($P < 0.05$) than DMSO-treated cells (2.58 ± 0.45). Similar data for thapsigargin, bortezomib, and rapamycin in treated U266 cells (4.57 ± 0.5, 4.14 ± 0.52, and 5.78 ± 0.5, respectively, $n = 50$) showed a significant increase ($P < 0.05$) in autophagosomes versus DMSO-treated cells (2.79 ± 0.42). Figure 1B shows representative assays showing the increase in punctate LC3-GFP detection in drug-treated U266 cells. A more detailed dose-dependent analysis of bortezomib-induced autophagy in U266 cells is shown in Fig. 1C, showing significant increases ($P < 0.05$) in autophagic area (*black columns*) and number of autophagosomes/cell (*white columns*) at all concentrations of bortezomib.

The above data showed increases in the number and area of autophagosomes. However, these increases could result from either an induced block in later autophagy events that cause accumulation of autophagosomes or from a true increase in flux through the autophagy pathway. As described (31), when GFP-LC3 is delivered to the lysosome, the LC3 part of the fusion protein is sensitive to proteolytic degradation but the GFP portion is resistant. Thus, the appearance of free GFP on Western blots can be used to monitor lysis of the autophagosome membrane and degradation of its cargo. As shown in Fig. 1D, treatment of 8226 or U266 cell lines with bortezomib resulted in generation of free GFP, best seen at 10 nmol/L drug concentration after 14 and 24 hours of incubation with 8226 cells and after 14 hours of incubation with U266 cells. An additional marker of increased autophagic flux is diminished p62 expression, as p62 becomes incorporated into the completed autophagosome and is degraded in autolysosomes (31). As shown in Fig. 1E, p62 became down-regulated in a time- and concentration-dependent fashion during exposure of MM cells to bortezomib. These data confirm that the increase in LC3-GFP signals is due to a true stimulation of autophagic flux induced by bortezomib rather than a block in later autophagy events.

Further confirmation of autophagy induction was obtained by electron microscopy. Autophagy was assayed by blindly counting the number of identified autophagosomal vacuoles. These vacuoles could be easily identified as shown in Fig. 2A and B (shown by *arrows*, high-power view in Fig. 2B). All three of the drugs were capable of increasing autophagy in 8226 cells assessed by electron microscopy as shown in Fig. 2C. Thapsigargin markedly and significantly ($P < 0.05$) increased the number of identified autophagosomal vacuoles from a mean of 5 ± 1 per cell (mean ± SD of 20

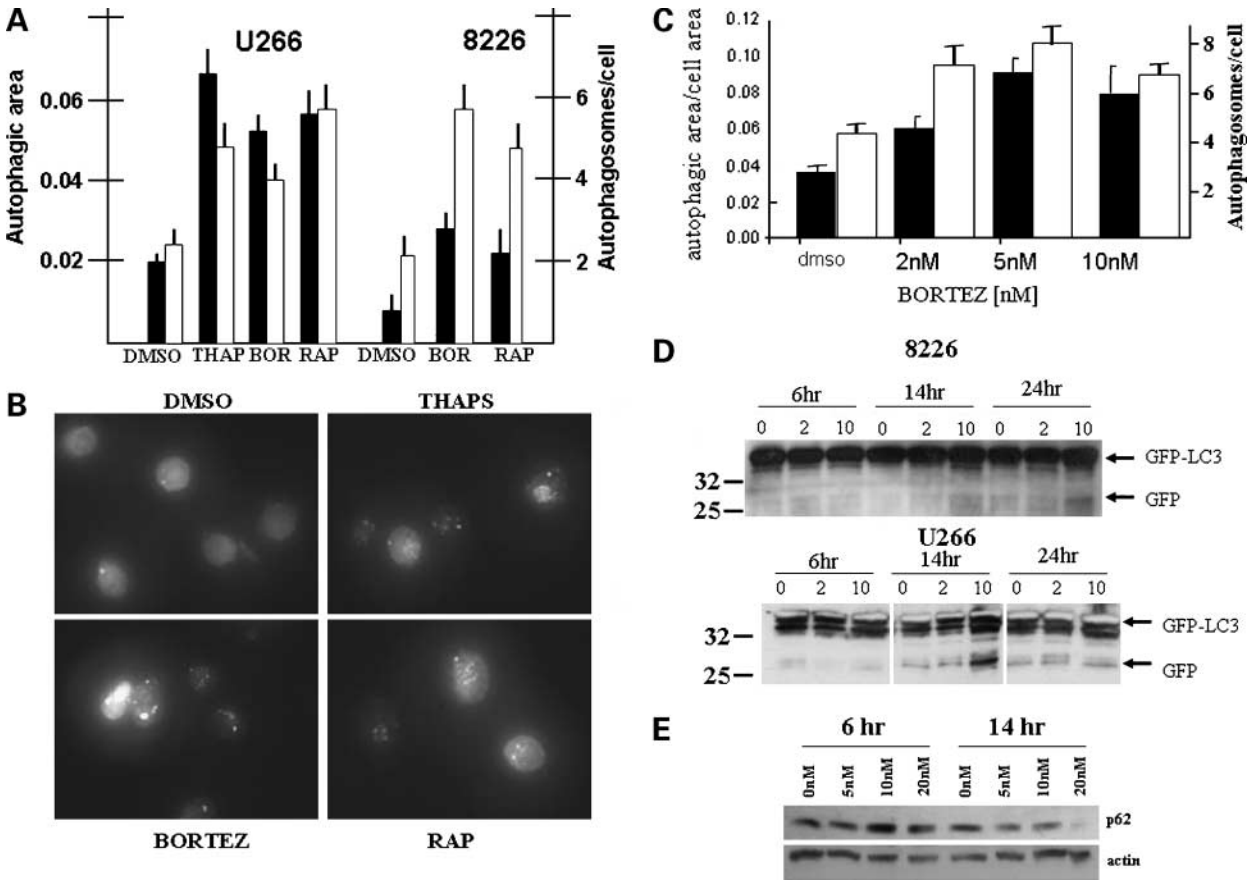

Figure 1. Assessment of myeloma cell autophagy by LC3 fluorescence. U266 and 8226 cell lines were stably transfected with GFP-LC3 and autophagic area/cell was determined as described in Materials and Methods. **A,** cells were treated with DMSO (control), thapsigargin (*THAP*; at 1 μmol/L), bortezomib (*BOR*; at 2 nmol/L), or rapamycin (*RAP*; at 100 nmol/L) for 24 h. Data presented as autophagy area/cell (*black columns*; $n = 3$) or number of autophagosomes/cell (*white columns*; $n = 45$–50). *Columns,* mean; *bars,* SD. Statistically significant increases over DMSO control, $P < 0.05$, were seen with all drug treatments for both autophagic area and number of autophagosomes/cell. **B,** representative pictures are shown of the GFP-LC3–expressing U266 MM cell following treatment with DMSO, thapsigargin (*THAPS*), bortezomib (*BORTEZ*), or rapamycin. Microscopic visualization is with a Leica Leitz DMRBE microscope at ×400 magnification and images were captured with a Hamamatsu C4742 camera and OpenLab program 3.1.5 software. **C,** autophagic area/cell (*black columns*) is presented in U266 cells treated with 0, 2, 5, or 10 nmol/L of bortezomib. *Columns,* mean ($n = 3$); *bars,* SD. *White columns,* number of autophagosomes/cell. Statistically significant increases ($P < 0.05$) over DMSO controls were seen at all concentrations of bortezomib. **D,** GFP-LC3–transfected 8226 or U266 cell lines treated with 0, 2, or 10 nmol/L of bortezomib for 6, 14, or 24 h and Western blot done for free GFP versus GFP fused to LC3. **E,** U266 cells exposed to increasing concentrations of bortezomib for 6 or 14 h and Western blot done for p62 and actin expression.

cells analyzed) to a mean of 17 ± 3 per cell (examples in Fig. 2A). Bortezomib also significantly increased the number of vacuoles/cell (12 ± 2 per cell versus 5 ± 1, $n = 20$, $P < 0.05$) and rapamycin modestly increased the number (11 ± 2 versus 5 ± 1, $n = 20$, $P < 0.05$).

During autophagy, LC3 is processed from the cytosolic form, LC3-I, to the membrane-bound form, LC3-II, and this can be detected by immunoblot (30). Our immunoblot assay for expression of endogenous LC3 confirmed the ability of thapsigargin, rapamycin, and bortezomib to induce autophagy (data not shown for rapamycin). As shown in Fig. 2D for OPM-2 and U266 cell lines, there is a dose-dependent increase in expression of LC3-II induced by bortezomib in both cell lines. Figure 2E also shows the inability of dexamethasone at 10^{-6} mol/L and melphalan at 5 and 20 μmol/L to induce autophagy in 8226 cells (with positive induction by thapsigargin), although they decreased viable cell recovery by 50% (comparable with thapsigargin in this experiment) and induced significant apoptosis (data not shown) in the same cells. This rules out the possibility that autophagy induction in MM cells is a nonspecific response to any agent capable of inducing MM cell injury and/or death. Figure 2F shows the ability of thapsigargin and bortezomib at 2, 5, 10, 20, or 50 nmol/L to enhance autophagy (LC3-II expression) in primary myeloma cells. Rapamycin at 10 nmol/L had only a minimal effect in one patient. Thus, specific induction of autophagy in MM cell lines and primary samples was detected following exposure to a proteasome inhibitor (bortezomib) and an ER stress inducer (thapsigargin). A mTOR inhibitor (rapamycin) was also capable of modest induction in MM cell lines, but more studies are needed to determine whether this drug can stimulate autophagy in primary samples.

Effects of Autophagy Inhibition on MM Cell Cytotoxicity

To test whether autophagy helps maintain viability in MM cells, we first used 3-methyladenine (3-MA) and chloroquine, known inhibitors of autophagy. 3-MA is a class III phosphatidylinositol 3-kinase inhibitor that prevents autophagy at the earliest stage of autophagosome formation (32) and was studied at concentrations (1, 5, or 10 mmol/L) known to inhibit autophagy in other cell models. As shown in Fig. 3A (*left*), 3-MA used at 1, 5, or 10 mmol/L induced a dose-dependent decrease in cell recovery (*white columns*) and viability (*black columns*) in all three cell lines (U266, 8226, and OPM-2 as noted in Fig. 3A). This cytoreductive effect roughly correlated with the ability of 3-MA to inhibit autophagy. Autophagy was monitored in U266 and 8226 cell lines by assessment of autophagosome area/cell as previously described in Fig. 1 and presented in Fig. 3A as percentage of control autophagy. In the OPM-2 line, which could not be transfected with LC3-GFP, effects on autophagy were monitored by immunoblot assay. As shown, a decreased LC3-II expression resulting from 5 and 10 mmol/L exposure to 3-MA identified inhibition of autophagy, which roughly correlated with inhibitory effects on cell recovery and viability.

Chloroquine, a weak base, concentrates in acidic vesicles such as lysosomes and disrupts vesicular acidification, a process that prevents fusion of autophagosomes with lysosomes, resulting in inhibition of autophagy (33, 34). By preventing autophagosome-lysosome fusion, chloroquine leads to accumulation of LC3-II in treated cells. Thus, immunoblot assays were used to assess chloroquine effects on autophagy

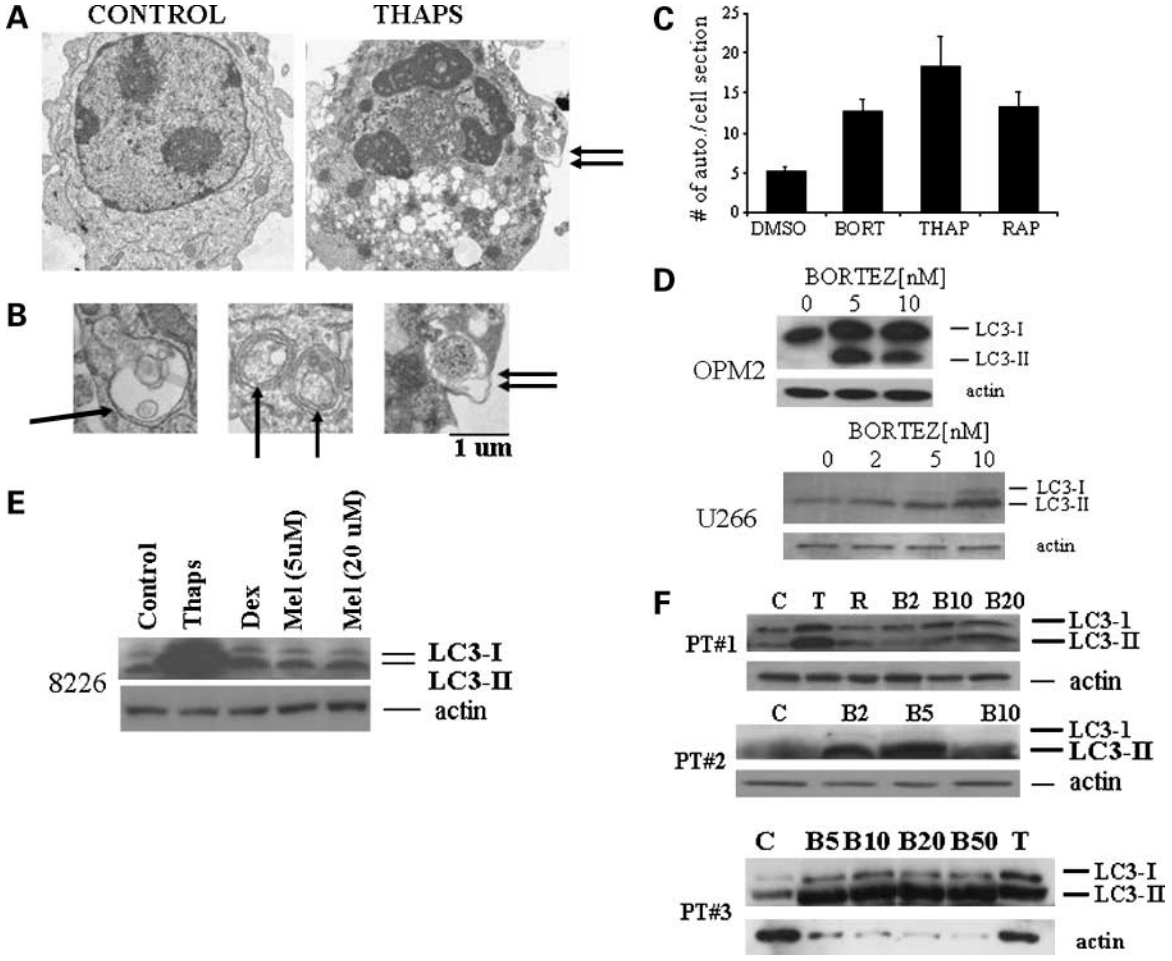

Figure 2. Assessment of myeloma cell autophagy by electron microscopy and LC3 immunoblot assay. **A** and **B,** electron microscopy done on U266 MM cells treated with DMSO (control), thapsigargin, bortezomib, or rapamycin for 24 h. Drug concentrations were as shown in Fig. 1. Arrows show areas of autophagosomes in **A** in thapsigargin-treated cells and higher-powered views in **B**. The high-power view of an autophagosome with double arrows in **B** is the identical structure shown in **A** with double arrows. **B,** magnification, 1 μm. **C,** the number of autophagosomes/cell is presented following 24-h incubation in DMSO, bortezomib (*BORT*), thapsigargin, or rapamycin. Concentrations as in Fig. 1. *Columns,* mean ($n = 20$); *bars,* SD. *, $P < 0.05$, statistically significant increases in autophagosomes over DMSO control. **D,** MM cell lines are treated with increasing concentrations of bortezomib for 24 h after which immunoblot is done for LC3-I, LC3-II, and actin expression. **E,** similar immunoblot assay is done after treatment of 8226 cells with thapsigargin (1 μmol/L), dexamethasone (*Dex*; 10^{-6} mol/L), or melphalan (*Mel*) at 5 or 20 μmol/L for 24 h. **F,** three primary MM specimens were incubated in medium [control (*C*), thapsigargin (*T*; 1 μmol/L), rapamycin (*R*; 100 nmol/L), or bortezomib (*B*; 2, 5, 10, 20, or 50 nmol/L)] for 24 h followed by immunoblot assay.

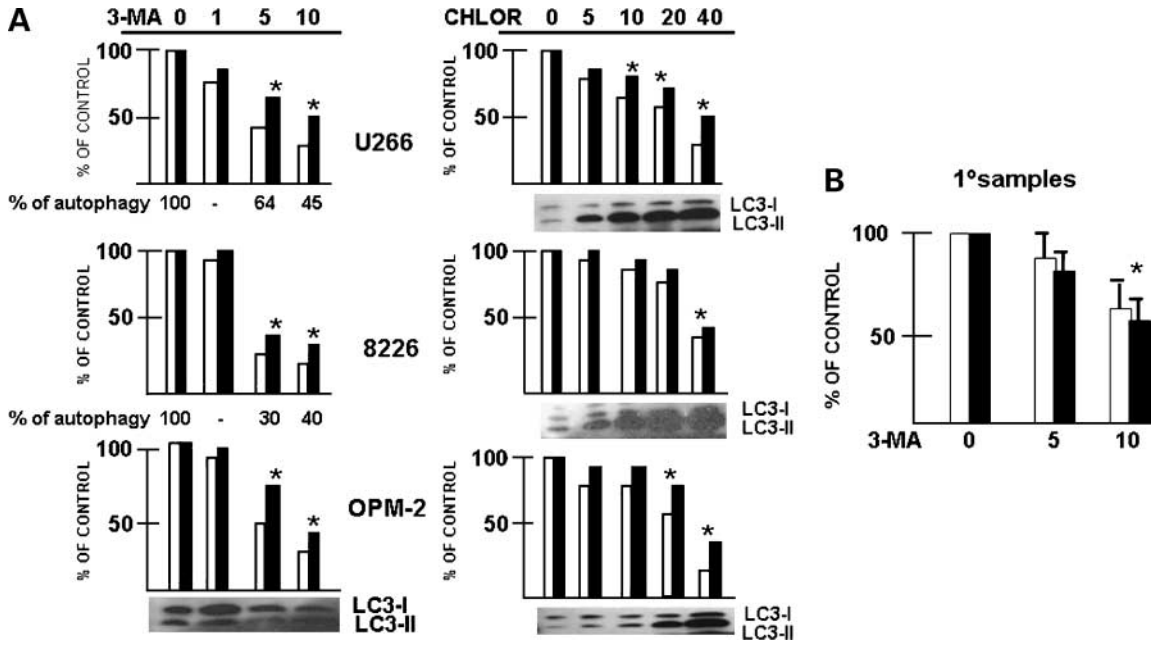

Figure 3. Inhibition of autophagy induces MM cell cytotoxicity. **A,** U266, 8226, or OPM-2 cells are treated for 24 h with 3-MA at 0, 1, 5, or 10 mmol/L or chloroquine (*CHLOR*) at 0, 5, 10, 20, or 40 μmol/L. Viable MM cell recovery was ascertained by trypan blue exclusion and presented as means of three separate experiments where all SDs were <5% of the respective means. Inhibition of autophagy by 3-MA was evaluated by inhibition of GFP-LC3 punctate fluorescence compared with control (0 concentration of 3-MA, 100% autophagy). Inhibition of autophagy was also evaluated in 3-MA–treated OPM-2 cells as well as chloroquine-treated cell lines by immunoblot analysis of LC3-I and LC3-II expression. *, $P < 0.05$, statistically significant decreases in viable recovery. **B,** three primary MM samples were treated for 24 h (*white columns*) or 48 h (*black columns*) with either 0, 5, or 10 mmol/L of 3-MA and viable cell recovery was assessed by trypan blue exclusion. *Columns,* mean ($n = 3$); *bars,* SD. *, $P < 0.05$, statistically significant decreases in viable recovery.

(Fig. 3A, *right*), with an increase in LC3-II levels reflecting inhibition. As shown, chloroquine, used at 5, 10, 20, or 40 μmol/L, reduced MM cell recovery and viability in all three cell lines. This was most evident at the chloroquine concentration of 40 μmol/L. This correlated well with effects on LC3-II accumulation in OPM-2 cells. However, with U266 and 8226 cell lines, there was significant LC3-II accumulation at lower chloroquine concentrations, which had insignificant or only modest effects on cell survival.

A limited number of flow cytometric analyses for apoptosis, using an antibody to activated caspase-3, showed that induction of apoptosis occurred in these experiments with autophagy inhibitors (in Supplementary Fig. S1).[1] For example, the percentage of U266 cells staining positive for activated caspase-3 following incubation in complete medium was 2 ± 2 (mean ± SE of three separate experiments), whereas exposure to 3-MA at 5 mmol/L resulted in 16 ± 4% positive staining and incubation in 10 mmol/L resulted in 36 ± 6%. A comparable induction of apoptosis was seen in 8226 cells treated with autophagy inhibitors (in Supplementary Fig. S1).[1]

A similar loss of viability and recovery was seen in primary MM samples (Fig. 3B). Three primary samples were incubated with 0, 5, or 10 mmol/L 3-MA for 24 hours (*white columns*) or 48 hours (*black columns*). A significant inhibition of viable MM cell recovery was identified at the 10 mmol/L concentration ($P < 0.05$). In at least one of these primary samples, we could show induction of apoptosis (Supplementary Fig. S1).[1]

To further identify autophagy as a possible survival-promoting mechanism in MM cells, we knocked down the *beclin-1* gene with siRNA in the U266 cell line. Beclin is the mammalian homologue of ATG 6, which is found in a complex with class III phosphatidylinositol 3-kinase and which is required for autophagy (35, 36). Beclin-1 siRNA was introduced into these cells by electroporation (Amanxa technique), which, in our hands, results in >80% transduction efficiency. As shown in Fig. 4A, siRNA was successful in knocking down expression of beclin-1. This knockdown muted the increase in autophagic cell area induced by bortezomib or thapsigargin (Fig. 4B). It also modestly muted the down-regulated expression of p62 induced by bortezomib (Fig. 4C). Finally, the viable recovery of beclin knocked down U266 cells was significantly decreased relative to control cells electroporated with a scrambled sequence (Fig. 4D). These gene knockdown data support the above results that use the 3-MA and chloroquine chemical inhibitors.

Combination Therapy

The induction of autophagy during treatment with bortezomib may have therapeutic implications. Because proteasome inhibition might injure MM cells via an increase in malfolded Ig, if autophagy was an additional mechanism available to the plasma cell for dealing with these toxic molecules, concurrent autophagy inhibition might result in synergistic antimyeloma effects. Thus, U266, 8226,

[1] Supplementary material for this article is available at Molecular Cancer Therapeutics Online (http://mct.aacrjournals.org).

and OPM-2 cell lines were concurrently treated with bortezomib ± chloroquine. As shown in Fig. 5, bortezomib alone showed a dose-dependent effect, with 8226 being the most sensitive line. The sensitivity of the lines to chloroquine was similar to previously shown data in Fig. 3A with 40 μmol/L having the greatest effect. Interestingly, the combination of bortezomib with chloroquine was consistently antagonistic with the greatest antagonism seen with low concentrations of both drugs. The CIs for drug combinations are shown to the right of the survival data with CI values >1 reflecting antagonism. A similar antagonistic interaction was seen when low concentrations of both drugs were used sequentially (2 hours before treatment with chloroquine followed by bortezomib; Supplementary Fig. S2).[1] CI values were also indicative of antagonism when the 3-MA inhibitor was used concurrently with bortezomib. With the U266 cell line, 3-MA at 5 mmol/L combined with bortezomib at 5 nmol/L resulted in a CI of 3, whereas 3-MA at 10 mmol/L combined with bortezomib at 10 nmol/L resulted in a CI of 1.9.

A similar antagonism was seen when both drugs were used concurrently against three primary samples (Fig. 6A). Bortezomib, used alone, showed significant antimyeloma activity against the primary specimens when used at 5 or 10 nmol/L. Likewise, 3-MA, when used alone, showed modest cytotoxic effects in all three patients (approximately 20–40% loss of survival at 10 mmol/L 3-MA compared with nontreated controls). However, combining bortezomib with 3-MA resulted in viable recovery of MM cells in all three specimens, which was higher than calculated from simple addition of the cytotoxic effects of each drug used separately. For example, in patient 1, 5 nmol/L bortezomib induces remarkable cytotoxicity by itself, resulting in ~90% loss of survival. Although 3-MA used alone at 5 and 10 mmol/L shows modest cytotoxic effects, combining them with bortezomib produces a significantly less toxic effect than achieved by bortezomib alone.

Further support for an antagonistic effect between autophagy inhibition and proteasome inhibitors was shown by combining beclin-1 siRNA with bortezomib (Fig. 6B). U266 cells electroporated with siRNA for beclin-1 show ~25% loss of viability (versus control scrambled sequence), whereas 10 nmol/L bortezomib induces 50% cytotoxicity. However, combining beclin-1 knockdown with bortezomib results in only 32% cytotoxicity (68% of control viability).

In contrast to this antagonism, when the autophagy inhibitor 3-MA was combined with thapsigargin, synergistic cytotoxicity was shown. As shown in Fig. 6C, U266 cells treated with 5 and 10 mmol/L 3-MA by itself show a decrease of 20% and 30% viable recovery, respectively, whereas thapsigargin at 1 μmol/L induces a 15% loss of viable recovery. However, combining thapsigargin with 10 mmol/L 3-MA results in a 60% decrease in viable recovery, which is greater than the sum of each treatment used separately (15% decrease with thapsigargin + 30% decrease with 3-MA). The synergy is even more obvious when these treated cells were analyzed for apoptosis by flow cytometry for activated caspase-3 (Fig. 6C, *bottom*). As shown, thapsigargin (1 μmol/L) induced ~10% apoptosis, whereas 3-MA used alone at 5 or 10 mmol/L induced 8% and 14% apoptosis, respectively. Combining thapsigargin with 3-MA at 5 and 10 mmol/L

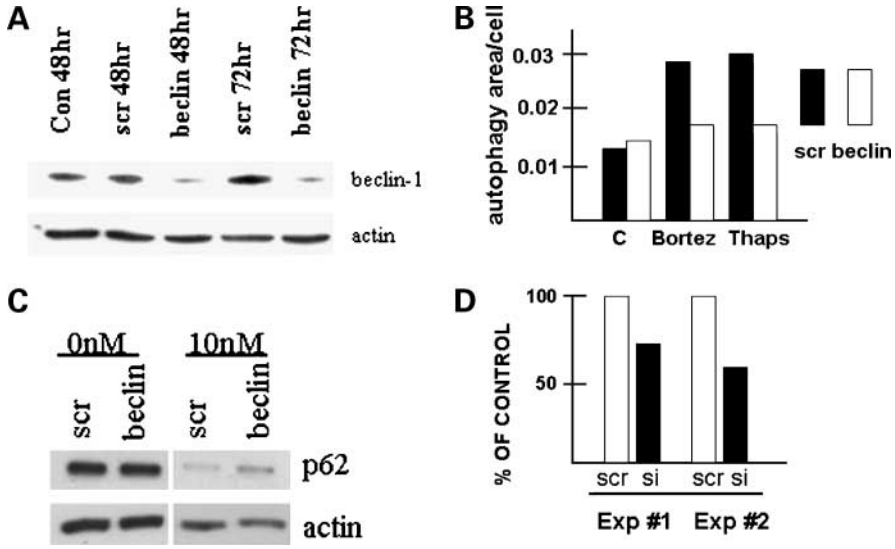

Figure 4. Effects of beclin-1 knockdown. **A,** the *beclin-1* gene was knocked down by siRNA in U266 cells as shown in the immunoblot assay (*Con 48hr*, nonelectroporated cells at 48 h; *scr 48hr* and *scr 72hr*, cells electroporated with scrambled control sequence 48 and 72 h after electroporation, respectively; *beclin 48hr* and *beclin 72hr*, cells electroporated with beclin siRNA). **B,** GFP-LC3–transfected U266 cells electroporated with scrambled sequence (*scr, black columns*) or beclin-1 siRNA (*beclin, white columns*) were treated with or without bortezomib (*Bortez*) or thapsigargin (*Thaps*) for 18 h and autophagic area/cell was assessed. **C,** scrambled (*scr*) or beclin-1 siRNA (*beclin*) transfected into U266 cells, which were then treated overnight with 0 or 10 nmol/L of bortezomib, and Western blot done for p62 expression. **D,** two separate experiments done where beclin siRNA (*si*) caused a decreased recovery of cells versus scrambled sequence (*scr*)–transfected cells [68% and 58% of control (scrambled sequence–electroporated cells), respectively].

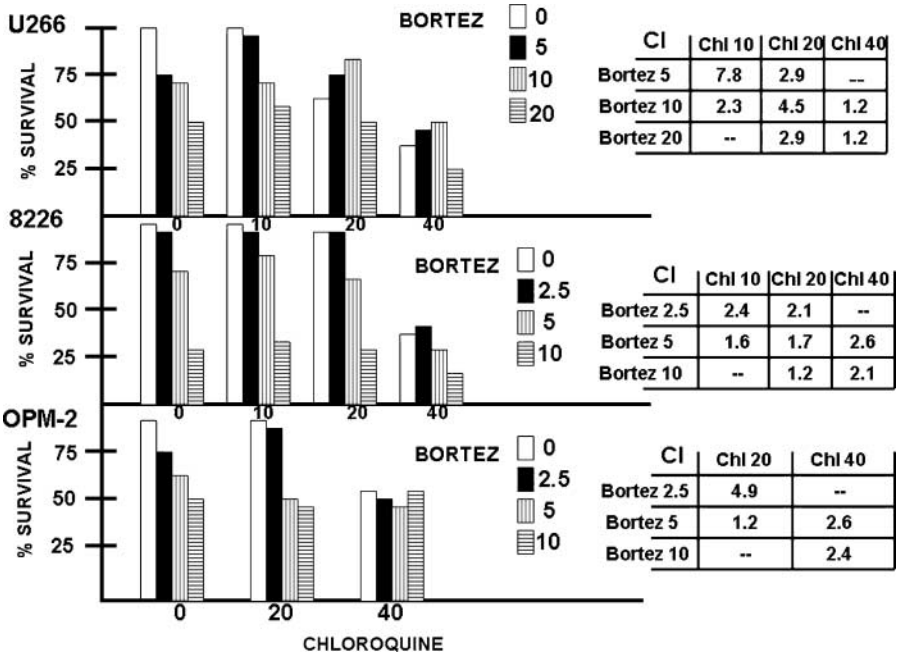

CI	Chl 10	Chl 20	Chl 40
Bortez 5	7.8	2.9	--
Bortez 10	2.3	4.5	1.2
Bortez 20	--	2.9	1.2

CI	Chl 10	Chl 20	Chl 40
Bortez 2.5	2.4	2.1	--
Bortez 5	1.6	1.7	2.6
Bortez 10	--	1.2	2.1

CI	Chl 20	Chl 40
Bortez 2.5	4.9	--
Bortez 5	1.2	2.6
Bortez 10	--	2.4

Figure 5. Combination therapy with bortezomib + chloroquine. U266, 8226, or OPM-2 cell lines were treated with increasing concentrations of chloroquine (0, 10, 20, or 40 μmol/L) in combination with increasing concentrations of bortezomib (0, 2.5, 5, 10, or 20 nmol/L). Data presented as percentage survival relative to nontreated cells (100%), means of four experiments where SDs were always <5% of the means. *Right,* CI values for the various combinations between chloroquine (*Chl*) and bortezomib.

induced 35% and 55% apoptosis, confirming a synergistic interaction.

One potential explanation for an antagonistic interaction between bortezomib and autophagy inhibitors is that a component of bortezomib-induced MM cell death is actually mediated by an autophagic pathway. To provide some support for that possibility, we exposed MM cell lines to toxic concentrations of bortezomib in the presence of ZVAD, which would prevent caspase-mediated apoptosis. As shown in Fig. 6D for U266 cells, ZVAD used at 20 or 40 μmol/L prevented bortezomib-induced caspase-3 cleavage (48-hour incubations). Nevertheless, a significant amount of ZVAD-resistant MM cell death was still induced (Fig. 6D). ZVAD-resistant cell death could be type II autophagic death, which would explain the previously shown antagonism between bortezomib and autophagy inhibitors.

Discussion

This study was prompted by previous literature, which suggested that targeting pathways that defend myeloma cells against the cytopathic effect of malfolded protein could be effective therapy. A huge amount of monoclonal Ig is synthesized by MM cells every day, invariably resulting in huge amounts of malfolded protein that must be cleared. Myeloma cells have developed efficient proteasome- and aggresome-dependent mechanisms for this process as well as a very efficient UPR cascade. The latter functions to temporarily decrease Ig synthesis and increase protein chaperone expression. Malfolded protein that overwhelms chaperone and proteasome capacity becomes aggregated and is gathered in aggresomes by a highly coordinated process. These aggresome structures may function as proteolysis centers specialized in degrading aggregated proteins or as collection centers for degradation by an autophagic pathway. Supporting the latter role for autophagy in degrading toxic aggregated proteins comes from studies (15–17) on degradation pathways for proteins implicated in neurologic disease such as α-synuclein (in Parkinson's disease; ref. 15) and huntingtin (in Huntington's disease; ref. 17). However, studies on a role for autophagy in protection of myeloma cell viability have not been previously done. Our studies show that basal autophagy protects MM cell viability and that autophagy is further enhanced by exposure of MM cells to ER stress inducers, proteasome inhibitors, and mTOR inhibitors. Unexpectedly, we also found that combining autophagy inhibitors with bortezomib resulted in antagonistic cytotoxic effects.

Autophagy was induced in MM cell lines and primary samples by exposure to rapamycin, a mTOR inhibitor, bortezomib, a clinically relevant proteasome inhibitor, and thapsigargin, a drug that induces ER stress by altering calcium metabolism. mTOR is a known inhibitor of autophagy, possibly working through its phosphorylation of ribosomal protein S6 (27, 37). Thus, we were not surprised to identify activation of autophagy in MM cells exposed to rapamycin. Recent work (19, 20, 38) indicates that stimulation of the UPR can activate autophagy. It is likely that this explains the induction of autophagy by thapsigargin. It is also possible that bortezomib induces autophagy by a

similar pathway. The UPR consists of three signal cascades activated when the ER reaches a threshold amount of malfolded protein. Although Lee et al. (4) described the ability of proteasome inhibitors to suppress the activity of IRE1-α, an initiator of one of the three cascades, with subsequent impairment of XBP-1 splicing in MM cells, Obeng et al. (3) documented that bortezomib activated other components of the terminal UPR cascade, including PERK, the eIF2α kinase. As eIF2α phosphorylation can mediate an essential step for autophagy formation (20), bortezomib-induced PERK activation could explain its ability to enhance autophagy. An ER stress–induced activation of JNK is also possible as a mechanism by which autophagy is stimulated (19) and bortezomib has been previously shown to activate JNK (39). In data not shown, bortezomib treatment of our MM cell lines was effective in inducing eIF2α phosphorylation and JNK activation, supporting these hypotheses. A recent publication (40) shows that proteasome inhibitors activate autophagy in colon cancer cells by a JNK-dependent pathway, further supporting this notion.

Our data support the notion that autophagy protects MM cell viability. Two independent inhibitors of autophagy, 3-MA and chloroquine, with different structures and different mechanisms of action, induced myeloma cell death of cell lines and primary specimens in a dose-dependent fashion. In addition, inhibition of autophagy, mediated by beclin-1 knockdown, also was cytotoxic to the U266 MM cell line. These data are consistent with prior work that underscored autophagy as a viability protector in cells stressed by nutrient deficiency (33, 41) or by ER stress (19, 20, 42). The induction of MM cell death was apoptotic in nature (type I programmed cell death) as shown by staining for activated caspase-3. This apoptotic response is also consistent with the above prior work on the role of autophagy during nutrient deficiency or ER stress. It is possible that the basal ongoing ER stress in these MM cell lines that synthesize Ig is sufficient to sensitize them to enhanced apoptosis if autophagy is inhibited.

Because of these viability-promoting effects of autophagy, we anticipated that cotreatment of MM cells with bortezomib and autophagy inhibitors would result in synergistic cytotoxic effects. In fact, two recent studies presented in abstract form (43, 44) suggest that synergy could be achieved in MM cells. In contrast, however, we were surprised to find an antagonistic effect of combined treatment. This suggests either that some of the cytotoxic effect of bortezomib against MM cells is mediated via autophagy or that the proteasome inhibitors and autophagy inhibitors use similar or overlapping pathways for cytotoxicity such that pathway stimulation by one agent can cancel out stimulation by the other

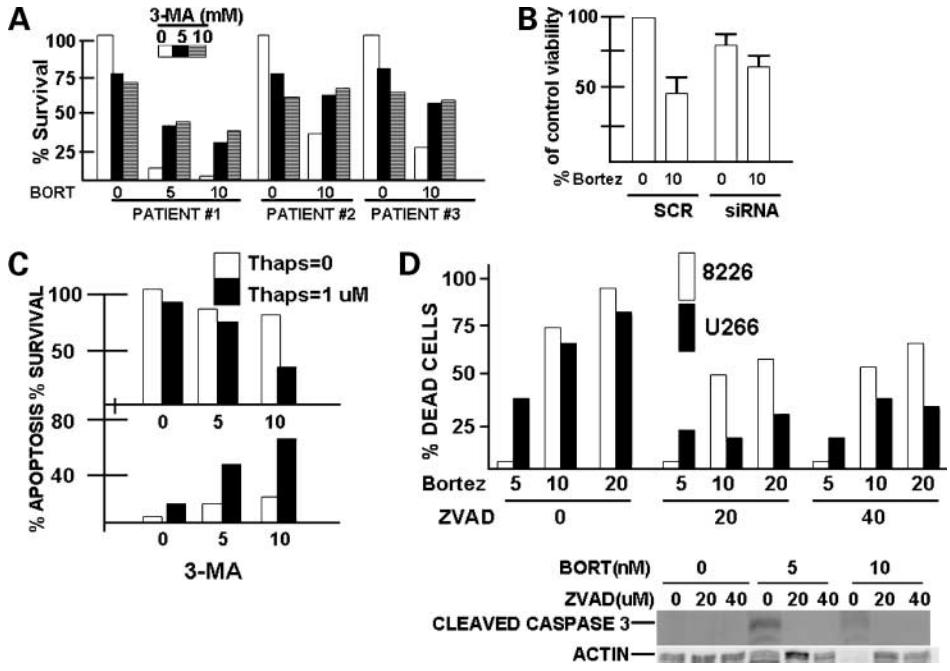

Figure 6. Effect of autophagy inhibition on bortezomib-treated primary cells or thapsigargin-treated cell lines. **A,** three primary samples were treated for 24 h with increasing concentrations of bortezomib (0, 5, or 10 nmol/L) combined with increasing concentrations of 3-MA (0, 5, or 10 mmol/L). Percentage survival was assessed relative to nontreated controls (100% survival). **B,** U266 cells were electroporated with beclin-1 siRNA or scrambled control sequence (*SCR*). Twenty-four hours later, electroporated cells were treated with or without bortezomib at 10 nmol/L for 24 h and viable recovery was determined. *Columns,* mean ($n = 3$); *bars,* SD. **C,** U266 cells were treated with increasing concentrations of thapsigargin (0 or 1 μmol/L) combined with increasing concentrations of 3-MA (0, 5, or 10 mmol/L) for 24 h, after which percentage survival was assessed (*top*, where control nontreated cells are 100% survival) or percentage apoptosis was assessed by flow cytometric analysis for activated caspase-3 (*bottom*). Results are means of three separate experiments. **D,** 8226 or U266 cells exposed to ZVAD at 0, 20, or 40 μmol/L in combination with bortezomib at 0, 5, 10, or 20 nmol/L. After 48 h, percentage cell death was analyzed by trypan blue exclusion and immunoblot on cell extracts for expression of cleaved caspase-3 or actin.

when both are used in combination. Some support for the former contention comes from experiments shown in Fig. 6D where significant bortezomib-induced death was independent of caspase cleavage and possibly mediated by type II autophagic cell death. At 20 and 40 μmol/L of ZVAD, caspase-3 cleavage induced by bortezomib was abrogated but a significant amount of cell death was still identified. Similar antagonistic results with combinations of proteasome inhibitors (MG132) and autophagy inhibitors (3-MA) were obtained by Yang et al. (45) where combined treatment of prostate cancer cells resulted in an inhibited cytotoxic response. Furthermore, the concept that excessive induction of autophagy could be a mechanism of MM cell death (instead of a protector against death) is supported by a recent article (46) in which an inhibitor of SCF^{Skp2}, which stabilized p21/p27, induced caspase-independent MM death, which was mediated by autophagy. However, when we combined an autophagy inhibitor with thapsigargin, we detected synergistic MM cell death. As noted in Figs. 1A and 2C, thapsigargin induced a greater degree of autophagy than bortezomib. Thus, it is more likely that it is the context of the enhanced autophagy (i.e., in the presence of proteasome inhibition or pure ER stress) rather than the degree of autophagy induction that determines its contribution to ultimate MM cell viability.

In summary, our data show that autophagy is significantly enhanced in MM cells exposed to ER stress inducers, mTOR inhibitors, and proteasome inhibitors. Constitutive autophagy seems to be a prosurvival mechanism in MM cells and could be a potential target of novel therapies. However, caution should be used before attempting combination therapy with newer autophagy inhibitors and proteasome inhibitors.

Disclosure of Potential Conflicts of Interest

No potential conflicts of interest were disclosed.

Acknowledgments

We thank Myrna Fisher for assistance with flow cytometry and the following University of California at Los Angeles core labs of the Jonsson Cancer Center: Janis Giorgi Flow Cytometry Laboratory and Microscopic Technique and Electron Microscopy Core Facility.

References

1. Hideshima T, Bradner JE, Chauhan D, Anderson KC. Intracellular protein degradation and its therapeutic implications. Clin Cancer Res 2005; 11:8530–3.

2. Mitsiades C, Mitsiades N, McMullan CJ, et al. Antimyeloma activity of heat shock protein-90 inhibition. Blood 2006;107:1092–100.

3. Obeng EA, Carlson LM, Gutman DM, Harrington WJ, Lee KP, Boise LH. Proteasome inhibitors induce a terminal unfolded protein response in multiple myeloma cells. Blood 2006;107:4907–16.

4. Lee A, Iwakoshi NN, Andeson KC, Glimcher LH. Proteasome inhibitors disrupt the unfolded protein response in myeloma cells. Proc Natl Acad Sci U S A 2003;100:9946–51.

5. Landowski T, Megli CJ, Nullmeyer KD, Lynch RM, Dorr RT. Mitochondrial-mediated disregulation of Ca^{2+} is a critical determinant of Velcade (PS-341/bortezomib) cytotoxicity in myeloma cell lines. Cancer Res 2005;65:3828–36.

6. Catley L, Weisberg E, Kizitepe T, et al. Aggresome induction by proteasome inhibitor bortezomib and α-tubulin hyperacetylation by tubulin deacetylase (TDAC) inhibitor LBH589 are synergistic in myeloma cells. Blood 2006;108:3441–9.

7. Maiso P, Carvajal-Vergara X, Ocio EM, et al. The histone deacetylase inhibitor LBH589 is a potent antimyeloma agent that overcomes drug resistance. Cancer Res 2006;66:5781–9.

8. Hideshima T, Richardson P, Chauhan D, et al. The proteasome inhibitor PS-341 inhibits growth, induces apoptosis and overcomes drug resistance in human multiple myeloma cells. Cancer Res 2001;61:3071–6.

9. Richardson P, Barlogie B, Berenson J, et al. A phase 2 study of bortezomib in relapsed, refractory multiple myeloma. N Engl J Med 2003;348: 2609–17.

10. Meister S, Schubert U, Neubert K, et al. Extensive immunoglobulin production sensitizes myeloma cells for proteasome inhibition. Cancer Res 2007;67:1783–92.

11. Hippert MM, O'Toole PS, Thorburn A. Autophagy in cancer: good, bad or both. Cancer Res 2006;66:9349–51.

12. Levine B, Klionsky DJ. Development by self-digestion: molecular mechanisms and biological functions of autophagy. Dev Cell 2004;6: 463–77.

13. Yorimitsu T, Klionsky DJ. Autophagy: molecular machinery for self-eating. Cell Death Differ 2005;12 Suppl 2:1542–52.

14. Klionsky DJ. The molecular machinery of autophagy: unanswered questions. J Cell Sci 2005;118:7–18.

15. Cuervo AM, Stefanis L, Fredenburg R, Lansbury PT, Sulzer D. Impaired degradation of mutant α-synuclein by chaperone-mediated autophagy. Science 2004;305:1292–5.

16. Iwata A, Christianson JC, Bucci M, et al. Increased susceptibility to cytoplasmic over nuclear polyglutamine aggregates to autophagic degradation. Proc Natl Acad Sci U S A 2005;102:13135–40.

17. Ravikumar B, Vacher C, Berger Z, et al. Inhibition of mTOR induces autophagy and reduces toxicity of polyglutamine expansions in fly and mouse models of Huntington disease. Nat Genet 2004;36:585–95.

18. Travers KJ, Patil CK, Wodicka L, Lockhart DJ, Weissman JS, Walter P. Functional and genomic analyses reveal an essential coordination between the unfolded protein response and ER-associated degradation. Cell 2000; 101:249–58.

19. Ogata M, Hino S, Saito A, et al. Autophagy is activated for cell survival after endoplasmic reticulum stress. Mol Cell Biol 2006;26:9220–31.

20. Kouroku Y, Fujita E, Tanida I, et al. ER stress (PERK/eIF2α phosphorylation) mediates the polyglutamine-induced LC3 conversion, an essential step for autophagy formation. Cell Death Differ 2007;14:230–9.

21. Shi Y, Hsu J, Hu L, Gera J, Lichtenstein A. Signal pathways involved in activation of p70 and phosphorylation of 4E-BP1 following exposure of multiple myeloma tumor cells to IL-6. J Biol Chem 2002;277:15712–20.

22. Hu L, Shi Y, Hsu J, Gera J, Van Ness B, Lichtenstein A. Downstream effectors of oncogenic ras in multiple myeloma cells. Blood 2003;101: 3126–35.

23. Shi Y, Yan H, Frost P, Gera J, Lichtenstein A. Mammalian target of rapamycin inhibitors activate the AKT kinase in multiple myeloma cells by up-regulating the insulin-like growth factor receptor/insulin receptor substrate-1/phosphatidylinositol 3-kinase cascade. Mol Cancer Ther 2005;4:1533–40.

24. Yan H, Frost P, Shi Y, et al. Mechanism by which mTOR inhibitors sensitize multiple myeloma cells to dexamethasone-induced apoptosis. Cancer Res 2006;66:2305–13.

25. An J, Rettig M. Epidermal growth factor receptor inhibition sensitizes renal cell carcinoma cells to the cytotoxic effects of bortezomib. Mol Cancer Ther 2007;6:61–9.

26. Thastrup O, Cullen PJ, Drobak BK, Hanley MR, Dawson AP. Thapsigargin, a tumor promoter, discharges intracellular Ca stores by specific inhibition of the ER Ca2(+)-ATPase. Proc Natl Acad Sci U S A 1990;87: 2466–70.

27. Blommaart EF, Luiken JJ, Blommaart PJ, van Woerkom GM, Meijer AJ. Phosphorylation of ribosomal protein S6 is inhibitory for autophagy in isolated rat hepatocytes. J Biol Chem 1995;270:2320–6.

28. Frost P, Moatamed F, Hoang B, et al. *In vivo* antitumor effects of the mTOR inhibitor CCI-779 against human multiple myeloma cells in a xenograft model. Blood 2004;104:4181–7.

29. Paglin S, Lee NY, Nakar C, et al. Rapamycin-sensitive pathway regulates mitochondrial membrane potential, autophagy and survival in irradiated MCF-7 cells. Cancer Res 2005;65:11061–70.

30. Kabeya Y, Mizushima N, Ueno T, et al. LC3, a mammalian homologue of yeast Apg8p, is localized in autophagosome membranes after processing. EMBO J 2000;19:5720–8.

31. Klionsky DJ, Abeliovich H, Agostinis P, et al. Guidelines for the use and interpretation of assays for monitoring autophagy in higher eukaryotes. Autophagy 2008;4:151–75.

32. Seglen PO, Gordon PB. 3-Methyladenine; specific inhibitor of autophagic/lysosomal protein degradation in isolated rat hepatocytes. Proc Natl Acad Sci U S A 1982;79:1889–92.

33. Boya P, Gonzalez-Polo R, Casares N, et al. Inhibition of macroautophagy triggers apoptosis. Mol Cell Biol 2005;25:1025–40.

34. Yamamoto A, Tagawa Y, Yoshimori T, Moriyama Y, Masaki R, Tashiro Y. Bafilomycin A1 prevents maturation of autophagic vacuoles by inhibiting fusion between autophagosomes and lysosomes in rat hepatoma cell line H-4-II-E. Cell Struct Funct 1998;23:33–42.

35. Liang XH, Jackson S, Seaman M, et al. Induction of autophagy and inhibition of tumorigenesis by beclin 1. Nature 1999;402:672–6.

36. Kihara A, Kabeya Y, Ohsumi Y, Yoshimori T. Beclin-phosphatidylinositol 3-kinase complex functions at the *trans*-Golgi network. EMBO Rep 2001;2:330–5.

37. Schmeizle T, Hall MN. TOR, a central controller of cell growth. Cell 2000;103:253–62.

38. Yorimitsu T, Nair U, Yang Z, Klionsky DJ. Endoplasmic reticulum stress triggers autophagy. J Biol Chem 2006;281:30299–304.

39. Hideshima T, Mitsiades C, Akiyama M, et al. Molecular mechanisms mediating antimyeloma activity of proteasome inhibitor PS-341. Blood 2003;101:1530–4.

40. Ding W, Ni H, Gao W, et al. Linking of autophagy to ubiquitin-proteasome system is important for the regulation of endoplasmic reticulum stress and cell viability. Am J Pathol 2007;171:513–24.

41. Codogno P, Meijer AJ. Autophagy and signaling: their role in cell survival and cell death. Cell Death Differ 2005;12:1509–18.

42. Bernales S, McDonald KL, Walter P. Autophagy counterbalances endoplasmic reticulum expansion during the unfolded protein response. PLOS Biol 2006;4:2311–24.

43. Landowski T, Escalante AM, Jefferson A, Dorr RT, Lynch R. Inhibition of autophagy promotes bortezomib-mediated cell death in myeloma cells. Blood 2008;112:1259a.

44. Shen PYC, Divakaran S, Ponduru S, Vogl DT, Amaravadi RK, Bradner JE. The rationale for combined proteasome and autophagy inhibition in multiple myeloma established using novel translational platforms. Blood 2008;112:951a.

45. Yang W, Monroe J, Zhang Y, George D, Bremer E, Li H. Proteasome inhibition induces both pro- and anti-cell death pathways in prostate cancer cells. Cancer Lett 2006;243:217–27.

46. Chen Q, Xie W, Kuhn DJ, et al. Targeting the p27 E3 ligase SCF^{Skp2} results in p27- and Skp2-mediated cell-cycle arrest and activation of autophagy. Blood 2008;111:4690–9.